Pergamon

PII: S0191-8141(97)00021-7

Journal of Structural Geology, Vol. 19, No. 7, pp. 987 to 996, 1997

0191-8141/97 $17.00 + 0.00

Forward modeling of non-steady-state deformations and the 'minimum strain path'

HAAKON FOSSEN

Department of Geology, University of Bergen, Allégt. 41, N-5007 Bergen, Norway

and

BASIL TIKOFF

Department of Geology and Geophysics, University of Minnesota, Minneapolis, MN 55455, U.S.A.

(*Received* 25 *June* 1996; *accepted in revised form* 31 *January* 1997)

Abstract—Structural analyses of shear zones often rely on an assumption of steady-state behavior, i.e. that the ratio of pure shear strain rate(s) to simple shear strain rate(s) remains fixed throughout deformation. However, geological deformations are not necessarily steady state. Non-steady-state deformation paths can be theoretically modeled if certain deformation parameters, such as strain or offset, are specified. We have analyzed a two-dimensional case of specified offset and geometry, termed the minimum strain path. The minimum finite strain needed to produce a fixed offset across a shear zone is neither simple shear nor pure shear, but a combination of the two (the minimum strain path). If this deformation accumulates with a steady-state deformation, the kinematic vorticity number (W_k) of the minimum strain path varies with the amount of finite offset, although W_k approaches 0.7 at high offset values. Because of this relation between W_k and finite offset, the minimum strain path is better modeled as a non-steady-state deformation, in which case deformation history starts close to simple shear but rapidly changes to a more pure shear dominated deformation. It is expected that the minimum strain path is applicable to geological deformation zones with relaxed boundary conditions, such as basal parts of spreading nappes or extensional detachment systems. © 1997 Elsevier Science Ltd.

INTRODUCTION

The recognition that pure shear and simple shear are end-members in a spectrum of two-dimensional deformations has caused a re-evaluation of deformation paths in structural geology. Some attempts have been made to quantify deformation history of naturally deformed rocks (e.g. Passchier and Urai, 1988; Wallis, 1992). Such studies generally indicate that deformation occurred through some two-dimensional combination of simple shearing and pure shearing, which has been referred to as sub-simple shearing (Simpson and De Paor, 1993). This approach represents a useful development from considering deformation zones as zones of pure shear or simple shear. However, most analyses of deformation are based on the assumption of steady-state deformation. The reason for this is the problem of retrieving information about deformation history from naturally deformed rocks. Future development would therefore not only involve expansion to three-dimensional non-coaxial deformation analyses, but also explore non-steady-state conditions.

Steady-state deformation requires that flow parameters such as the velocity field, flow apophyses, kinematic vorticity number (W_k) and infinitesimal strain axes (ISA) do not change during deformation (e.g. Bobyarchick, 1986). In general, however, a given state of finite strain can be produced by an infinite number of non-steady-state deformation histories, and retrieving deformation histories from naturally deformed rocks is very difficult. The steady-state alternative therefore serves as a useful reference deformation path in lack of a better alternative. Consequently, some workers have quantified deformation history of naturally deformed rocks through the use of an average kinematic vorticity (W_n) (e.g. Passchier and Urai, 1988; Wallis, 1992). However, non-steady-state deformation can be modeled in the forward sense if the changing boundary conditions of deformation are specified.

The best indication of steady-state deformation is perhaps one of constant boundary conditions. For instance, if the relative motion between two plates is constant over an extended period, then the resulting deformation zone may approximate steady-state behavior (e.g. Tikoff and Fossen, 1995). However, there is no *a priori* reason to believe that geological deformation is steady state, and there are many deformation settings that intuitively should *not* enhance steady state. These include cases involving anisotropic volume loss related to compaction, which occurs early in the deformation history, or to metamorphic reactions, which depend on fluid availability, and P–T conditions that are likely to change during deformation. External causes, such as changing boundary conditions, would also result in non-steady-state deformation. A large-scale example of the latter is where the relative motion between two colliding plates changes, either gradually or instantaneously during a deformation history. In this manuscript, we present a method of forward modeling in order to model non-steady-state deformation. In particular, we explore

the 'minimum strain path', which is a sub-simple shear deformation that minimizes strain with respect to displacement.

CHARACTERIZING NON-STEADY-STATE DEFORMATION

Characterization of non-steady-state deformation requires the knowledge of the velocity field at every time interval during deformation. A velocity field is defined by the velocity gradient tensor **L**, which contains components of the stretching (**S**) and vorticity (**W**) tensors, such that

$$\mathbf{L} = \mathbf{S} + \mathbf{W}.$$

Steady flow implies that **L** does not change with time (e.g. Means, 1995) and that the acceleration in the shear zone is not a major factor (e.g. Jiang, 1994; Ishii, 1995). The vorticity component (**W**) can be subdivided into internal or shear-induced vorticity, caused by simple shearing, and external vorticity or spin, where the ISA rotate with respect to an external frame (e.g. Lister and Williams, 1983). Since only the internal vorticity is recorded within a shear zone (or any volume of homogeneously deformed rock), we will only address this quantity in our calculations. For ductile shear zones, the orientation of the shear-zone boundaries is assumed to be fixed. In other words, although the entire shear zone can rotate in space, we will keep our reference as the shear-zone boundary and not include external spin in vorticity calculations.

The velocity field, flow apophyses, infinitesimal strain axes (ISA) and kinematic vorticity number (W_k; see Means *et al.*, 1980 and Tikoff and Fossen, 1995 for a closer treatment) can be defined as *infinitesimal deformation parameters*, because their orientations and magnitudes are only given at a single instant or for infinitely short period and will change during non-steady deformation (Tikoff and Fossen, 1995; Passchier and Trouw, 1996). The flow apophyses are given as the eigenquantities (eigenvalues and eigenvectors) of **L**, the ISA as the eigenquantities of **S**, and W_k is a function of all components of **L**. If deformation proceeds in a steady-state manner, the infinitesimal deformation parameters can be deduced from the orientation of the finite deformation parameters (Vissers, 1989; Passchier, 1990; Wallis, 1992; Fossen and Tikoff, 1993; Ishii, 1995). Figure 1 illustrates these deformation parameters.

Non-steady-state deformation occurs if the boundary conditions (Fig. 1) change during deformation. In this case, the orientation of most of the infinitesimal deformation parameters are likely to change as well (Fig. 1). Further, the orientation of the infinitesimal deformation parameters can no longer be deduced from the orientation of the finite deformation parameters. Rather, the finite deformation parameters show a more complex pattern, which is still potentially useful in determining strain history within the shear zone.

A special case of non-steady-state plane-strain deformation involves only changes in the pure shear/simple shear ratio (sub-simple shear), where the eigenvectors of both flow *components* have fixed orientations throughout deformation. For simplicity, this is the only type of deformation that will be considered in this paper. First, we analyze sub-simple shear as a steady-state deformation. Further, we will address non-steady-state by quantifying changes in W_k during sub-simple shearing. W_k is an infinitesimal quantity, recording the relative rates of rotation to stretching (e.g. Means *et al.*, 1980; Tikoff and Fossen, 1995), and its value will change during non-steady-state deformation. In two dimensions, W_k can be considered as a non-linear relation between the pure shear and simple shear components of deformation (Tikoff and Fossen, 1995), with $W_k = 1$ implying simple shear and $W_k = 0$ implying pure shear flow. Additionally, the orientation of the ISA depend on W_k, as does the angle between the two flow apophyses (e.g. Bobyarchick, 1986). Thus, ISA and flow apophyses can also be used to quantify two-dimensional non-steady-state deformation.

MODELING STRAIN HISTORY: THE MINIMUM STRAIN PATH

The accumulation of finite strain in non-steady-state (and steady-state) deformations can easily be done with a computer, for example by adding small increments of deformation, each of which involves a slightly different W_k. The problem with this approach is that one must assign a kinematic history to the shear zone. Therefore, rather than constructing a completely arbitrary non-steady-state history for a deforming zone, it is appropriate to construct a geometric problem that utilizes non-steady-state deformation. In the example below, we use displacement and strain as parameters to construct such a geometric problem.

Strain and offset of geological markers are important concepts in structural geology, and are commonly obtainable from field observations. They are, for instance, important components in restoration and modeling of thrust systems, extensional shear zones and gravity spreading. It is generally assumed that pure shear is the least effective method of creating an offset, while simple shear is the most effective (Pfiffner and Ramsay, 1982). This may be one reason why simple-shear deformation is often assumed. Other reasons may be that simple shear is easy to handle, and lack of clear evidence of deviations from simple shear. However, it is possible to theoretically explore plane-strain combinations of simultaneous pure and simple shearing (sub-simple shearing of Simpson and De Paor, 1993) to investigate the relation of strain history to offset.

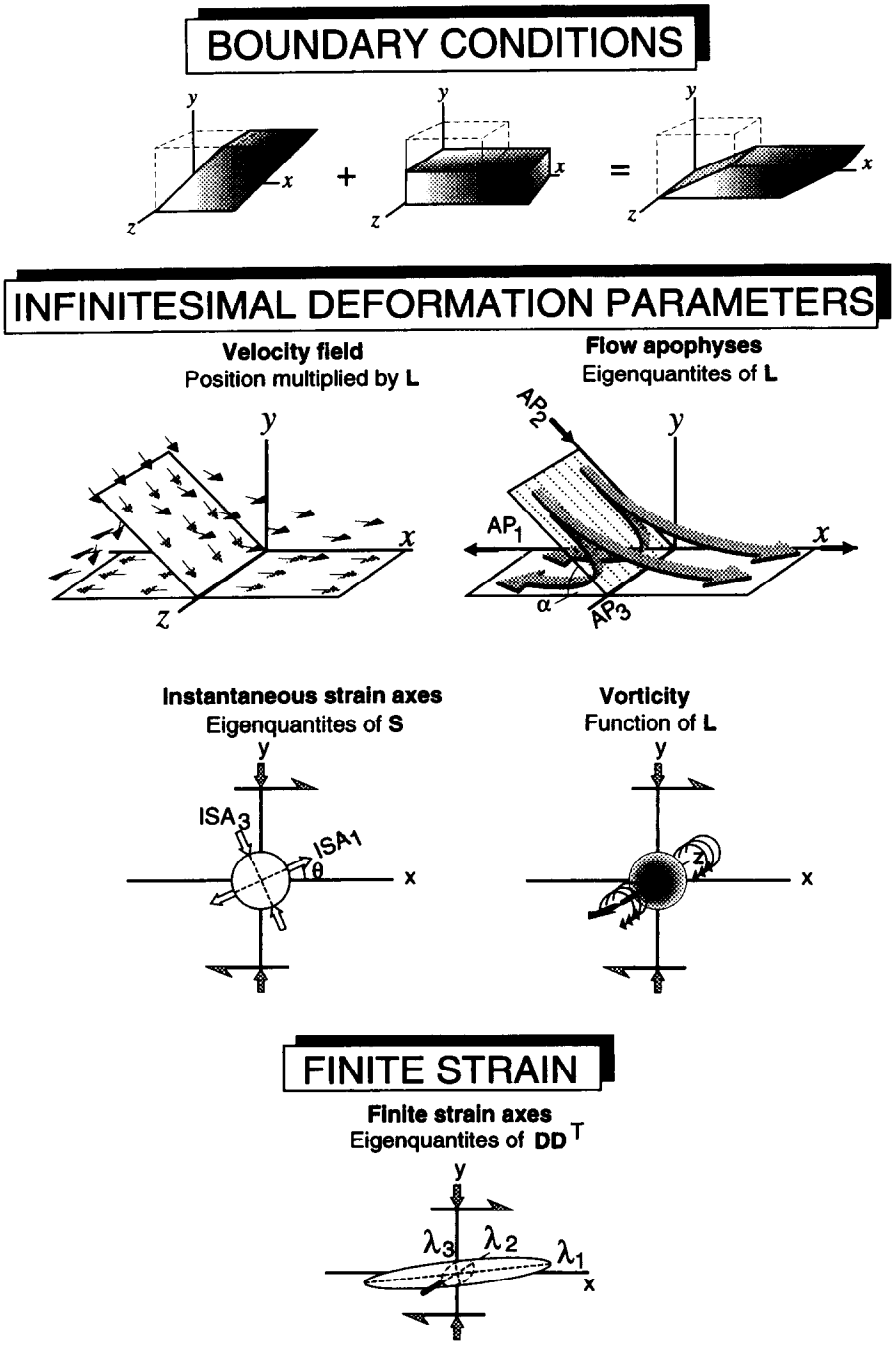

Fig. 1. Strain and flow parameters for sub-simple shearing (pure shear combined with a simple shear). Infinitesimal deformation parameters—the velocity field, flow apophyses (APs), infinitesimal strain axes (ISA) and kinematic vorticity—will all change during non-steady-state deformation. Finite deformation parameters (finite strain ellipsoid and its orientation) will integrate the entire deformation history.

Steady-state sub-simple shearing

Before modeling non-steady combinations of simple shear and pure shear, we consider steady-state sub-simple shearing deformations. In order to investigate this subject using a computer, we created a box, pinned the lower-left corner at the origin and offset the upper right-hand corner (Fig. 2). The horizontal offset was specified, but the vertical height could vary during deformation. Assuming steady-state deformation, the computer then checked all the possible W_k values to the nearest 0.001 and chose the W_k value that would *minimize* the finite strain ellipse for a specified horizontal offset of the upper, right-hand corner of the deforming box (Fig. 2). The

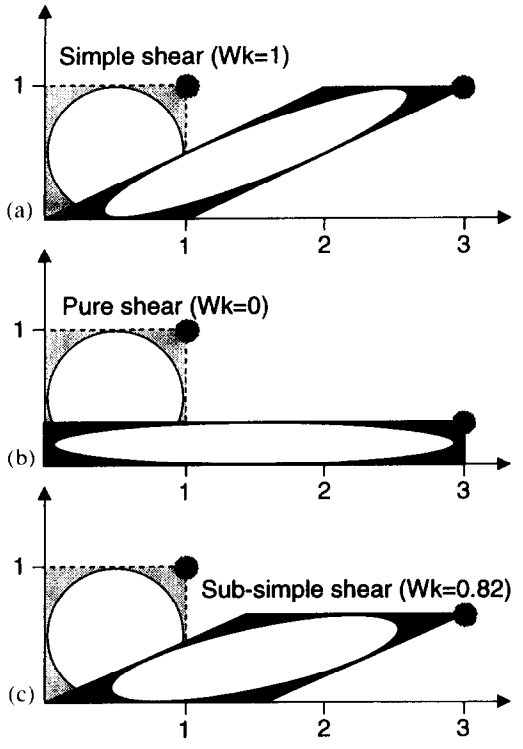

Fig. 2. Depiction of the finite strain ellipse for (a) simple shear, (b) pure shear and (c) sub-simple shear of $W_k = 0.82$ (the minimum strain path for offset = 2). For a prescribed offset of the upper, right-hand corner of the deforming box, the finite strain ellipse ratio is substantially smaller for the minimum strain path ($W_k = 0.82$) than for the two other deformation. For a prescribed strain, see Fig. 4.

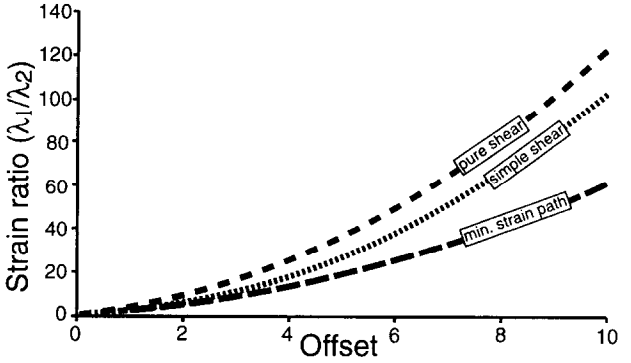

Fig. 3. Finite strain ratio vs offset for simple shear, pure shear and the minimum strain path. For a given offset, the finite strain is significantly less for the minimum strain path than for the other two deformations. The difference in finite strain increases as the offset gets larger. The minimum strain path applies to both the steady-state and non-steady-state deformations discussed in the text. Offset relates to upper right-hand corner of box in Fig. 2 and to black line marker in Fig. 4.

minimum strain path, i.e. the strain path that created the smallest finite strain, was thus calculated. Simultaneously, the path is also a maximum offset path if strain is specified.

The modeling demonstrated that simple shear produces a smaller finite strain than pure shear for an identical offset, but that the finite strain is minimized by a simultaneous combination of the two (minimum strain path, Fig. 2). In other words, for the specified geometry, simple shear is *not* the most effective strain history at accumulating offset for a given strain. For example, for an offset of 2, the finite strain ellipse ratio is higher for either pure shear or simple shear than for a combination of the two specified by $W_k = 0.82$ (Figs 2 and 3).

The relation between displacement, strain and deformation type is also illustrated in Fig. 4. Here, a rigid lower block is overlain by a deformable middle layer, and an upper block is allowed to deform if needed. Circles and vertical structures provide strain markers. In all of the deformed versions, the strain within the middle layer is the same (albeit with different orientations of the strain ellipse). Hence, the strain is specified here, whereas displacement was specified in Fig. 2.

Simple shear (Fig. 4b) produces a classical shear zone with undeformed upper and lower blocks. If pure shear is applied to the middle layer and the upper block, a basal slip surface develops and the total offset at the end of the system becomes larger (Fig. 4c). However, displacement decreases to the left, and the offset related to the black marker is less than for simple shear (Fig. 2). Displacement vanishes on the pinned left-hand side.

For a sub-simple shear with $W_k = 0.82$ (Fig. 4d), the black line is displaced considerably more than for simple shear (Fig. 4b) or pure shear (Fig. 4c). Because of the pure-shear component, displacement decreases to the left also in this case, but the simple-shear component causes displacement of the left-hand end of the upper block which is of comparable size to that in Fig. 4(b). The right-hand end is displaced considerably longer than both the simple shear (Fig. 4b) and pure shear (Fig. 4c) examples. This example shows how displacement is a relative parameter in deformation zones that deviate from simple shear, but that the minimum strain path generally provides larger displacements than both pure shear and simple shear.

A steady-state deformation of $W_k = 0.82$ corresponded to the minimum strain path for an offset of 2 of the upper right-hand corner in Fig. 2, or of the black marker in Fig. 4(d). For a larger or smaller offset, a different steady-state W_k value minimized the strain (Fig. 5, steady state). For example, the lowest strain was provided by a steady-state deformation with $W_k = 0.82$ for an offset of 2, $W_k = 0.74$ for an offset of 5 and $W_k = 0.72$ for an offset of 8.

Non-steady sub-simple shearing

With a steady-state deformation, as considered above, a rock would have to prejudge its final state to choose the correct W_k to maximize its offset—an unlikely event except for very clever rocks. Therefore, a non-steady-state approach was also simulated on the computer. We used the same setup as above, except that in this case an incremental (instead of final) offset was applied. The computer then checked all the possible W_k values to the nearest 0.0001 and chose the W_k value that would *minimize* the finite strain ellipse for a specified horizontal offset. This was done successively for each offset

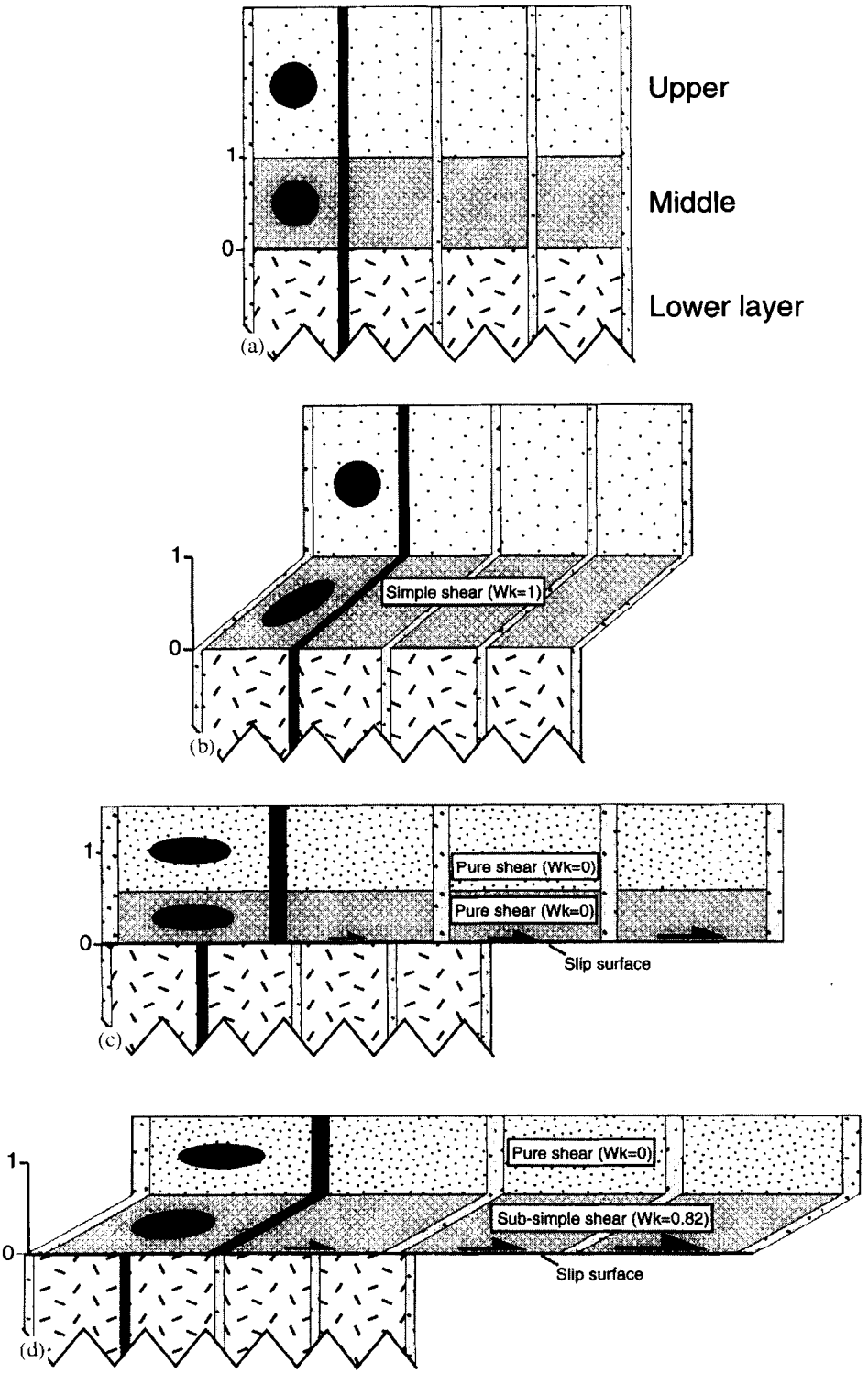

Fig. 4. (a) Three rock layers prior to deformation with circular and vertical strain markers. (b) Deformation of central layer by simple shear. (c) Deformation of both central and upper layer by pure shear. (d) Deformation of the central layer by sub-simple shear and the upper layer by pure shear. The strain in the central layer is equal for (b)–(d), while displacement is variable. The (pure shear) strain in the upper layer is different in (c) and (d) for compatibility reasons. In (c) and (d) a slip surface or stretching fault develops between the lower and middle layers. The total offset is clearly largest in (d). In the minimum strain path discussed in the text, we consider the displacement of the black marker, which is largest for sub-simple shear (d) and smallest for pure shear (c). Although applicable to any scale, the upper layers may be thought of as a nappe above an undeformed basement in (c) and (d).

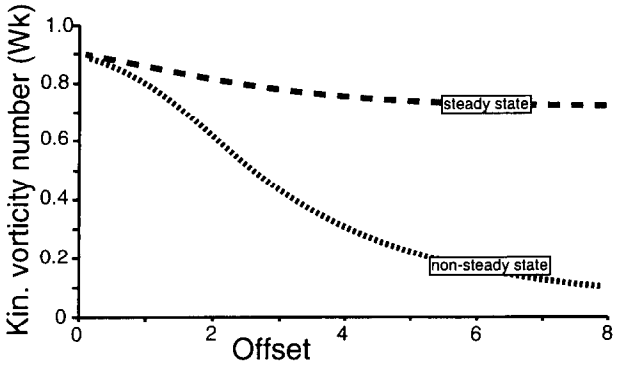

Fig. 5. The effect of offset (see Fig. 2) on kinematic vorticity for both steady-state and non-steady-state minimum strain path (sub-simple shearing). The steady-state W_k value, which stays fixed throughout the steady-state deformation history, is lower with increasing finite offset (i.e. each finite offset requires a different W_k). The non-steady-state path corresponds to a single strain history in which the W_k value decreases continuously. In this case W_k can be approximated by a vorticity function. The finite strain, for a given offset, is identical for the steady-state and non-steady-state paths.

increment 0.2 or less, with the initial shear zone width of 1.0. In order to model non-steady deformation, the W_k was allowed to change from one increment to the next.

The non-steady-state strain path started at $W_k = 0.89$ for the first increment of deformation, as did the steady-state minimum strain path (Fig. 5). However, for larger offsets the non-steady-state path decreases to $W_k = 0.10$, which is substantially lower than the deformation accumulated with a constant W_k value ($W_k = 0.72$). Hence, the deformation will start to accumulate with much simple shear and, as the accumulated offset becomes larger, a greater pure-shear component is needed to compensate for the early simple-shear deformation. For example, consider an offset of 2. If we consider a steady-state deformation, we find that $W_k = 0.82$ will minimize the finite strain. If we consider a non-steady-state deformation, the *average* W_k (W_n of Passchier, 1988) will also equal 0.82 (Fig. 2c). However, the non-steady-state deformation will start to accrue with almost simple shear ($W_k = 0.89$) and, as the offset becomes larger, a greater pure-shear component is needed to compensate for the early simple-shear deformation.

From the data (Fig. 5) we can approximately describe how W_k changes as displacement increases by the fourth-order polynomial vorticity function which best fits ($R^2 = 1$) the data:

$$W_k = 0.90538 + 0.6833d + 0.06220d^2 + 0.00136d^3 + 0.00080d^4,$$

where d is the finite displacement or offset across the zone.

It is important to realize that the finite strain ellipse, for a given offset, is identical for the non-steady-state (or 'incremental') path and the steady-state path (Fig. 2). The reason is that there is only one orientation and ellipticity of the finite strain ellipse that will maximize the offset, and the shear box can arrive at this position by either a steady-state path, a non-steady path that maximized offset at each step or even an infinite variety of other paths. Therefore, a steady-state $W_k = 0.82$ for an offset of 2 provides the same finite strain as a non-steady-state which starts at $W_{k\ \text{incremental}} = 0.89$ and decreases to $W_{k\ \text{incremental}} = 0.61$ (Fig. 5). It is important to note that although the finite strain is the same for the two cases, the deformation history is not.

Figure 6 is an attempt to explain the difference between steady-state and non-steady-state minimum strain paths by quantification of the orientation of the infinitesimal strain axes (ISA). Because the ISA are fixed for a particular steady-state deformation, an offset of 4 ($d = 4$; Fig. 6a) causes a fixed ISA oriented at 24.6° from the shear-zone boundary (and one of the flow apophyses). In contrast, the non-steady-state path starts with the ISA oriented at 31.4° from the shear-zone boundary ($W_k = 0.89$) and the ISA rotates progressively towards an angle of 8.8° ($W_k = 0.30$) as the offset approaches 4. The orientation of the ISA for the steady-state deformation must lie between the starting and ending ISA

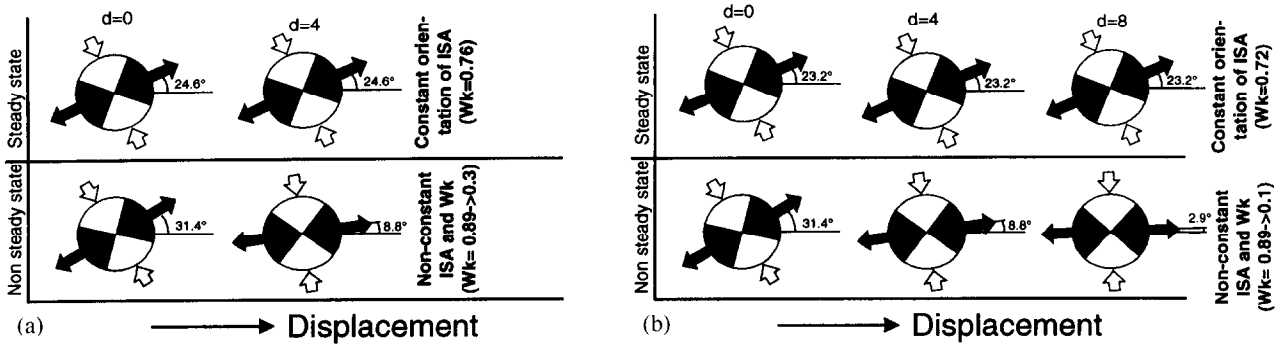

Fig. 6. An illustration of the difference between the steady-state and non-steady-state minimum strain paths using the orientation of the infinitesimal strain axes orientations for finite offset (d) of 4 in (a) and 8 in (b). In both cases, the steady-state deformation accumulates with a constant orientation of the ISA, but the orientation depends on the finite displacement (and W_k; see Fig. 5). The orientation of the ISA thus differs for the two offsets. The non-steady-state path always starts with the largest ISA oriented at 31.4°, but rapidly progresses to lower orientations with increasing offset.

orientations of the non-steady-state path. However, the orientation of the steady-state ISA is slightly closer to the simple-shear end-member of the non-steady path, because of the tendency of a pure-shear component of deformation to dominate the finite strain (e.g. Tikoff and Fossen, 1995). For a larger offset ($d=8$; Fig. 6b), there is a slightly increased pure-shear component of deformation. This is accommodated in steady-state deformation with the ISA oriented at 23.2° ($W_k=0.723$), i.e. slightly lower than the case of offset $d=4$. The non-steady-state path still starts with the ISA oriented at 31.4° ($W_k=0.89$), but the ISA rotates towards an angle of 2.9° ($W_k=0.10$). Again, the orientation of the ISA for the steady-state deformation lies between the starting and ending ISA orientations of the non-steady-state path.

As explained above, the minimum strain path can also be considered a maximum offset path for a given strain. For example, if a strain of 4:1 is recorded, the maximum offset of 5 occurs for a steady state $W_k=0.74$ or an average $W_n=0.74$ for a non-steady-state deformation. The offset is thus maximized for a combination of simple and pure shear, which implies that the pure-shear component adds significantly to the net displacement or translation of material above the deforming zone. Further, it is important to realize that the W_k is 'biased', so that a $W_k=0.74$ actually records an approximately equal effect of pure and simple shear on the infinitesimal deformation (Tikoff and Fossen, 1995).

DISCUSSION

Application of the minimum strain path requires that the deformation is approximated by two-dimensional, sub-simple shear and undergoes non-steady-state deformation. Further, the boundary conditions put restrictions to the nature of the geological setting. In general, two types of boundary conditions may exist for a zone where deformation follows a minimum strain path. In the first case, deformation is continuous across the sub-simple shear zone, as shown in Fig. 7(b). The pure-shear component of deformation requires that some elongation of the sub-simple shear zone must exist. If strain compatibility must be maintained, the pure-shear component that occurs in the deforming zone must also occur above and below the deforming zone (Fig. 7b & c).

Alternatively, the minimum strain path is also applicable to examples in which strain compatibility does not rigorously apply. Discontinuities, such as the existence of pervasively fractured rocks or upper and/or lower décollements (Fig. 7d & e), act to negate strain compatibility restrictions. If we relax the lower boundary condition to allow for discontinuous deformation, the lower block can be left undeformed. This would lead to a detachment or stretching fault (Means, 1989) between the sub-simple shear zone and the lower part of the section (Fig. 7d & e). If we relax both the upper and lower boundary conditions, both the upper and lower block remain undeformed, and an extruding zone develops in between.

Application to spreading–gliding thrust nappes

Potentially the best example of deformation that is not limited by strain compatibility constrictions is the gravitationally driven movement of ice sheets over bedrock. The bedrock–ice interface can be treated as a detachment, above which the ice is free to undergo any type of deformation. Many authors consider this situation analogous to gliding and spreading nappes in the upper to middle crust. Some of these (e.g. Ramberg, 1977, 1981, 1989, 1991; Merle, 1986, 1989) investigated cases of spreading nappes above décollement zones both numerically and experimentally. The kinematics of spreading–gliding nappes commonly indicate non-steady-state, sub-simple shear (e.g. Merle, 1986). Therefore, it is possible that the minimum strain path could describe deformation of this type of system.

The minimum strain path may also apply to nappes in general. A common observation in orogenic collision zones is a relatively undeformed basement below a major décollement zone (thin-skinned tectonics). In this example, the geometry can be accommodated by the creation of a basal thrust (stretching fault) between the undeformed basement and the sub-simple shear zone (Fig. 7e). Rigorous strain compatibility restrictions may not apply above a major basal thrust that reaches the surface of the earth (e.g. Sanderson, 1982). Therefore, the deformation within and structurally above a major thrust fault may well be influenced by pure shear, as predicted by the minimum strain path.

Application to crustal-scale extension

Another potential application of the minimum strain path involves extensional tectonics, particularly extensional collapse of gravitationally unstable areas. With a free upper surface and a flexible crust–mantle boundary, crustal-scale extensional collapse may not be strongly limited by strain compatibility requirements. A simplified model for crustal-scale deformation for this scenario involves an upper part which deforms brittlely (upper crust), a middle section (middle crust) which defines a sub-simple shear zone near the brittle–ductile transition (e.g. Miller *et al.*, 1983) and a lower part beneath the sub-simple shear zone (lower crust). There is no reason why the deformation within the middle to lower crust should be either simple shear or pure shear, or that deformation should be steady state. Instead, several authors have suggested that lower crustal extensional deformation is predominately by pure shearing (McKenzie, 1978; Hamilton, 1987; Andersen and Osmundsen, 1994) (Fig. 7c). Similarly, fault geometries in the upper crustal parts of rift systems often indicate overall pure shear. Interestingly, the model shown in Fig. 7(c) explains non-coaxial deformation underlain by a zone of contemporaneous

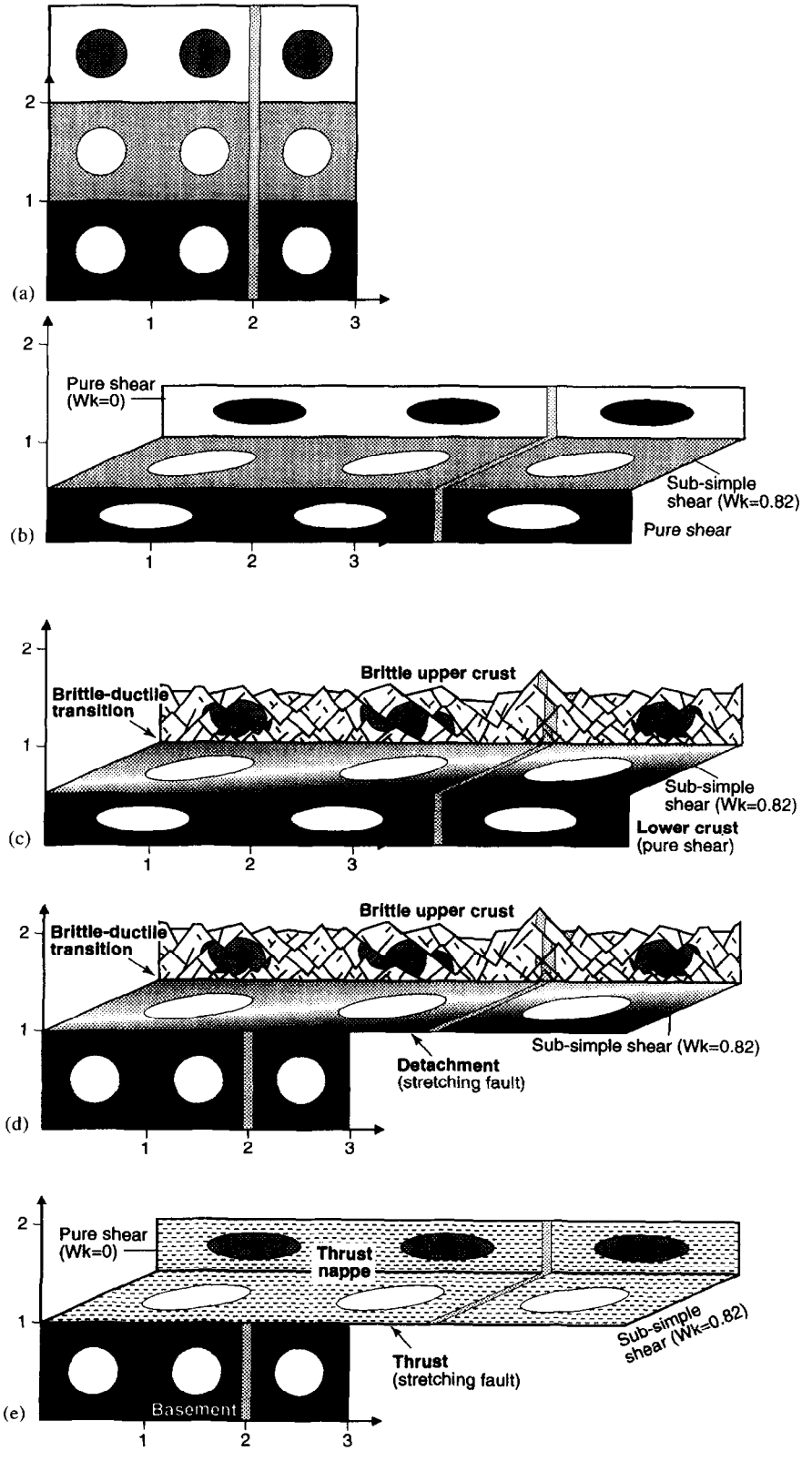

Fig. 7. Visualization of sub-simple-shear deformation zones in the crust, where deformation followed the minimum strain path. (a) shows the undeformed section. If strain compatibility must be maintained, the pure-shear component that occurs in the deforming zone must also occur both above and below the deforming zone (b and c). In (d) and (e) the lower section is undeformed, creating a slip surface or stretching fault (Means, 1989) between the basement and the shear zone. The upper part of (b) and (d) could represent a spreading nappe above a sub-simple shear zone (e.g. Ramberg, 1989, 1991). One could also envisage a crustal-scale model where the upper crust deforms brittlely above a sub-simple shear zone, and the lower crust deforms by pure shear, as illustrated in (c) and (e).

coaxial (pure-shear) deformation, whereas pure shear has sometimes been assumed to represent an earlier stage of extension in collapsed orogens (cf. Andersen and Osmundsen, 1994).

If we allow for discontinuous deformation along the lower boundary of the sub-simple shear zone, the lower block can be left undeformed. In an extensional setting, this would lead to a detachment or stretching fault (Means, 1989) between the sub-simple shear zone and the lower part of the section (Fig. 7d).

Application to fabric development

A shear zone that underwent a strain history given by the minimum strain path would undergo a dramatic change in W_k during deformation. This change may be reflected by the orientation and geometry (symmetry) at various stages of deformation. Thus, structural features that recorded either infinitesimal or small incremental deformation (e.g. tension gashes, fibers) would be biased towards the later, more coaxial, deformation. Likewise, there would be overprinting of earlier formed features formed under deformation conditions closer to simple shear. The resulting, composite fabrics could easily be interpreted as multiple episodes of deformation.

Comparison with Nadai's minimum work path

The minimum strain path is important because it exhibits that non-steady-state deformations are potentially important for geometric reasons and are easily forward-modeled with computers. However, in this context, it should be made clear that the minimum strain path differs significantly from Nadai's minimum work path (Nadai, 1963). Nadai's minimum work path investigates the minimum work for a ideally plastic substance to reach a final deformation. The minimum work path, similar to the minimum strain path, typically follows a non-steady-state path. For example, a final deformation that follows the minimum work path and results in a simple-shear deformation does not have a constant W_k value during deformation.

However, unlike the minimum strain path, the final deformation is not uniquely specified for the minimum work path (Nadai, 1963). Rather, a minimum work path exists for any finite deformation: a specified deformation that results in a finite strain ratio and orientation will have a specified minimum work path. As an example, a finite deformation that corresponds to a simple-shear deformation of $\gamma = 2$ will follow a non-simple shearing ($W_k \neq 1$) deformation path. Contrarily, the minimum strain path predicts the finite strain ratio and orientation, and the deformation is always sub-simple shearing.

CONCLUSIONS

Particularly questionable in most kinematic analyses of shear zones is the assumption of steady-state deformation. Steady-state deformation is especially problematic for strain histories involving deformation mechanisms that change during deformation or changing boundary conditions (such as plate motions). Non-steady-state deformations can easily be forward-modeled using computers, utilizing either knowledge of changing boundary conditions or geometric constraints of deformation. Using the latter approach, we have constructed a non-steady-state strain history for the minimum strain path. This strain history minimizes the finite strain accumulated during sub-simple shearing, for a predetermined offset of a marker. The kinematic history of this deformation is characterized by a relatively rapid change from simple shear dominated ($W_k \approx 0.9$) to a pure shear dominated shearing ($W_k \approx 0.1$). This change is expected to be reflected in fabrics formed at different stages during deformation. The minimum strain path may be applicable to gravitationally induced movement, and other flows which are not strongly limited by strain compatibility requirements. An important observation from the analysis is that the pure-shear component adds significantly to the net displacement or translation. Therefore, investigation of the minimum strain path indicates that some caution is required in balancing cross-sections in rift zones or nappe regions without considering internal deformation of the system (e.g. Mitra, 1994).

Acknowledgements—We are thankful for referee comments by C. W. Passchier and S. Wallis, which improved the contents of this contribution. This study was supported by an National Science Foundation EAR-9628381 grant for B. Tikoff. Financial support for the project was also provided by the University of Bergen (Bergen Museum).

REFERENCES

Andersen, T. B. and Osmundsen, P. T. (1994) Deep crustal fabrics and a model for the extensional collapse of the southwest Norwegian Caledonides. *Journal of Structural Geology* **16**, 1191–1203.

Bobyarchick, A. R. (1986) The eigenvalues of steady flow in Mohr space. *Tectonophysics* **122**, 35–51.

Fossen, H. and Tikoff, B. (1993) The deformation matrix for simultaneous simple shearing, pure shearing, and volume change, and its application to transpression/transtension tectonics. *Journal of Structural Geology* **15**, 413–422.

Hamilton, W. (1987) Crustal extension in the Basin and Range Province, southwestern United States. In *Continental Extensional Tectonics*, eds M. P. Coward, J. F. Dewey and P. L. Hancock, pp. 155–176. Geological Society of London Special Publication **28**.

Ishii, K. (1995) Estimation of non-coaxiality from crinoid-type pressure fringes: comparison between natural and simulated examples. *Journal of Structural Geology* **17**, 1267–1278.

Jiang, D. (1994) Vorticity determination, distribution, partitioning and the heterogeneity and non-steadiness of natural deformations. *Journal of Structural Geology* **16**, 121–130.

Lister, G. S. and Williams, P. F. (1983) The partitioning of deformation in flowing rock masses. *Tectonophysics* **92**, 1–33.

McKenzie, D. (1978) Some remarks on the development of sedimentary basins. *Earth and Planetary Science Letters* **40**, 25–32.

Means, W. D. (1989) Stretching faults. *Geology* **17**, 893–896.

Means, W. D. (1995) Shear zones and rock history. *Tectonophysics* **247**, 157–160.

Means, W. D., Hobbs, B. E., Lister, B. E. and Williams, P. F. (1980) Vorticity and non-coaxiality in progressive deformations. *Journal of Structural Geology* **2**, 371–378.

Merle, O. (1986) Patterns of stretch trajectories and strain rates within spreading–gliding nappes. *Tectonophysics* **124**, 211–222.

Merle, O. (1989) Strain models within spreading nappes. *Tectonophysics* **165**, 57–71.

Miller, E. L., Gans, P. B. and Garing, J. (1983) The Snake Range décollement: and exhumed mid-Tertiary ductile–brittle transition. *Tectonics* **2**, 239–263.

Mitra, G. (1994) Strain variation in thrust sheets across the Sevier fold-and-thrust belt (Idaho–Utah–Wyoming): implications for section restoration and wedge taper evolution. *Journal of Structural Geology* **16**, 585–602.

Nadai, A. (1963) *Theory of Flow and Fracture of Solids*. McGraw-Hill, New York.

Passchier, C. W. (1988) Analysis of deformation paths in shear zones. *Geologische Rundschau* 77, 309–318.

Passchier, C. W. (1990) Reconstruction of deformation and flow parameters from deformed vein sets. *Tectonophysics* **180**, 185–199.

Passchier, C. W. and Trouw, R. A. J. (1996) *Microtectonics*, 289 pp. Springer, Berlin.

Passchier, C. W. and Urai, J. L. (1988) Vorticity and strain analysis using Mohr diagrams. *Journal of Structural Geology* **10**, 755–763.

Pfiffner, O. A. and Ramsay, J. G. (1982) Constraints on geological strain rates: arguments from finite strain states of naturally deformed rocks. *Journal of Geophysical Research* **87**, 311–321.

Ramberg, H. (1977) Some remarks on the mechanism of nappe movement. *Geologiska Föreningensi Stockholm Förhandlingar* **99**, 110–117.

Ramberg, H. (1981) The role of gravity in orogenic belts. In *Thrust and Nappe Tectonics*, eds K. R. McClay and N. J. Price, pp. 125–140. Geological Society of London Special Paper **9**.

Ramberg, H. (1989) A new numerical simulation method applied to spreading nappes. *Tectonophysics* **162**, 173–192.

Ramberg, H. (1991) Numerical simulation of spreading nappes, sliding against basal friction. *Tectonophysics* **188**, 159–186.

Sanderson, D. J. (1982) Models of strain variations in nappes and thrust sheets: a review. *Tectonophysics* **88**, 201–233.

Simpson, C. and De Paor, D. G. (1993) Strain and kinematic analysis in general shear zones. *Journal of Structural Geology* **15**, 1–20.

Tikoff, B. and Fossen, H. (1993) Simultaneous pure and simple shear: the unified deformation matrix. *Tectonophysics* **217**, 267–283.

Tikoff, B. and Fossen, H. (1995) The limitations of three-dimensional kinematic vorticity. *Journal of Structural Geology* **17**, 1771–1784.

Vissers, R. L. M. (1989) Asymmetric quartz *c*-axis fabrics and flow vorticity: a study using rotated garnets. *Journal of Structural Geology* **11**, 231–244.

Wallis, S. R. (1992) Vorticity analysis in metachert from the Sanbagawa Belt, SW Japan. *Journal of Structural Geology* **14**, 271–280.